Protecting plants against the fungal pathogen *Sclerotinia sclerotiorum* using host-induced gene silencing

by

Rhey Caners

A thesis submitted to the Department of Biological Sciences, University of Manitoba,

in partial fulfillment of the requirements for the course

BIOL 4100 (Honours Thesis)

for the degree of

Bachelor of Science (Honours)

Abstract

Sclerotinia sclerotiorum is a fungal pathogen that affects Canadian crops every year. *Brassica napus* (canola) is particularly vulnerable. Chemical fungicides are widely used to control *S. sclerotiorum.* However, with increasing concerns about resistance and ecological effects, it is necessary to develop new and improved control methods. Host-induced gene silencing (HIGS) is an RNA interference technology that has the potential to be harnessed to create transgenic, pathogen-resistant crops. In this study, I analyzed the effectiveness of four independently transformed lines of *Arabidopsis thaliana* expressing RNA to silence the NOB1 gene (SS1G_07873) in *S. sclerotiorum.* Three of the lines expressed double-stranded (ds)RNA while the fourth line expressed paperclip (pc)RNA, a novel RNA structure which folds over itself on both ends to protect it from nucleases. The analysis was done through detached-leaf lesion assays and transcript knockdown analysis of the NOB1 target gene as well as three known interacting genes. Though improvements are required, the lesion assays show significant decreases in lesion size. Transcript knockdown analysis revealed insignificant changes in NOB1 expression. The interacting genes analyzed showed a significant reduction in transcript abundance, indicating that further experiments are required to understand the processing of foreign RNA in the plant. With further testing to optimize HIGS using SS1G_07873, this technology has the potential to be replicated in crop plants as a means of protection against *S. sclerotiorum.*

Acknowledgements

First, I would like to thank my supervisor, Dr. Mark Belmonte, for providing the opportunity to work in his lab and for the guidance I received throughout this project. I am grateful to lab members Yujia Wu, Lara Carroll, and Brigo Castillo for their mentorship and for sharing their time and expertise with me.

I would also like to thank committee member Dr. Steve Whyard for his supportive feedback and encouragement during the course of my honours year and to committee member Dr. Jae-Hyeok Lee for his thoughtful input.

Table of Contents

List of Tables

List of Figures

Introduction

Plants are susceptible to a broad range of pests and pathogens (Cai *et al.* 2011; MacLeod *et al.* 2010). Worldwide, there is a loss of 10-23% of crops pre-harvest and an additional 10-20% post-harvest due to fungal pathogens (Stukenbrock & Gurr 2023). The necrotrophic fungus, *Sclerotinia sclerotiorum* (white mold) is one of Canada's most economically devastating plant pathogens, affecting over 400 plant species across 75 families, including canola (*Brassica napus*) of which 41% of Manitoban fields were infected in 2022 (Boland & Hall 1994; Elmhirst 2023).

Due to staggering losses, farmers have turned to broad-spectrum fungicides to protect plants against fungal pathogens like *S. sclerotiorum*. This fungus is particularly difficult to eradicate due to the presence of long-term overwintering structures, termed sclerotia, which can remain dormant in the soil for years (Derbyshire & Denton-Giles 2016). Additionally, many strains of *S. sclerotiorum* have developed resistance to fungicides due to their long-term use (Duan *et al*. 2013; Wang *et al.* 2022; Zhou *et al*. 2014). Broad-spectrum fungicides can kill both pathogenic and advantageous fungi indiscriminately, as well as negatively affecting the health of pollinators (Yoder *et al.* 2017). Unlike other fungal pathogens, such as blackleg (*Leptosphaeria maculans*), *B. napus* lacks sufficient natural defenses to *S. sclerotiorum,* leaving the species vulnerable and the breeding of resistant cultivars remains inadequate (Derbyshire & Denton-Giles 2016; Zhang & Fernando 2018).

S. sclerotiorum exhibits a necrotrophic lifecycle with a brief initial biotrophic phase making its pathogenic interaction and the plant responses more complex (Kabbage *et al.* 2013). During initial infection, the fungus releases numerous cell-wall degrading enzymes and toxins, most notably, the phytotoxin oxalic acid (OA) which kills host cells and disrupts the plant's immune response (Dutton & Evans 1996; Riou *et al.* 1991; Williams *et al.* 2011). One of the

immune processes dampened by OA is the hypersensitive response (HR), characterized by the production of reactive oxygen species (ROS) (Mur *et al.* 2007; Williams *et al.* 2011). This suppression helps the fungus establish an infection and is characteristic of a biotrophic pathogen (Williams *et al.* 2011). After the establishment of infection, *S. sclerotiorum* transitions to a necrotrophic lifecycle by inducing ROS production and programmed cell death in the plant through the HR (Williams *et al.* 2011). As necrotrophs get energy from deceased or dying cells, the dead plant cells provide an additional growth substrate (Govrin & Levine 2000). In this way, *S. sclerotiorum* effectively uses a plant's immune system against them as they secrete virulence factors to promote the plant's HR (Ghozlan *et al.* 2020).

A method of controlling plant pathogens called host-induced gene silencing (HIGS) has been developed (Nowara *et al.* 2010). HIGS uses RNA interference (RNAi) where the host plant is genetically modified to produce complimentary small interfering RNAs (siRNA) for genes in a pathogen coding essential proteins or virulence factors which are then consumed by the pathogen (Andrade *et al.* 2015). Once inside the pathogen, the siRNA is processed by Dicer-like proteins into 21-24 nucleotide-long siRNA fragments (Bernstein *et al.* 2001; Wang *et al.* 2023). The siRNAs are unwound into two single-stranded fragments and the antisense strand is bound to an Argonaute protein to form an RNA-induced silencing complex (RISC) (Hammond *et al.* 2001). The RISC then targets complementary messenger RNA (mRNA) strands for degradation by slicing the mRNA with the endonucleolytic activity of Argonaut (Hammond *et al.* 2000; Liu *et al.* 2004). The slicing and degradation of the mRNA stops the translation of the protein that the

targeted mRNA codes for (figure 1).

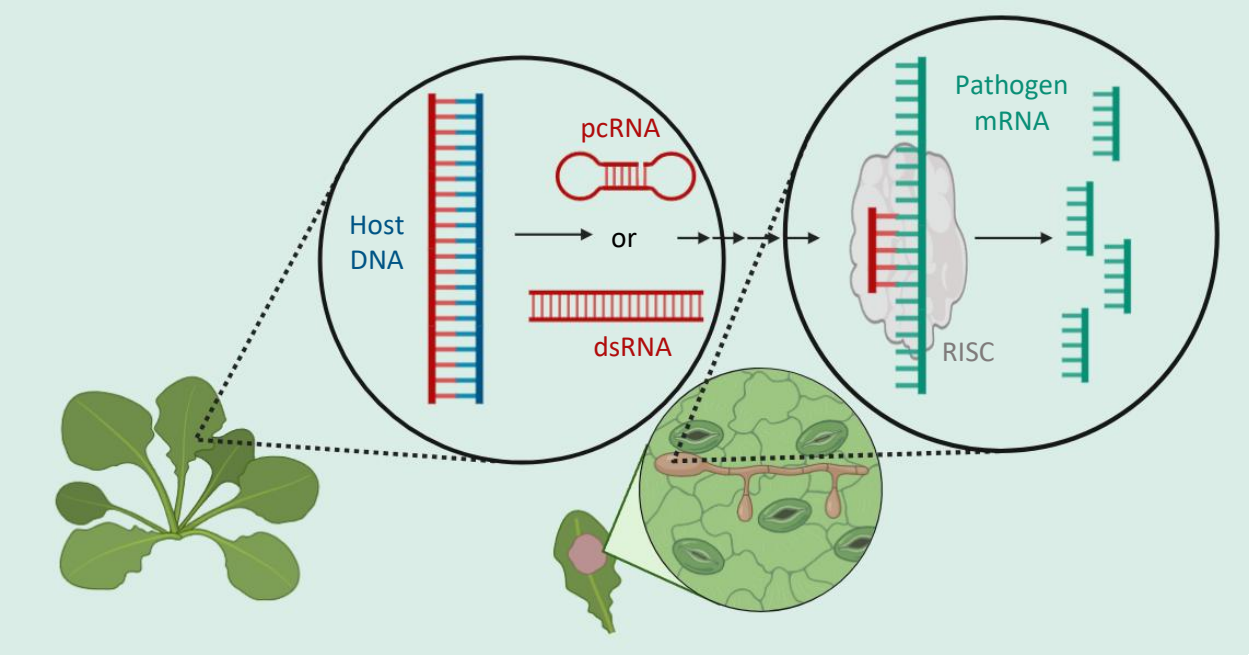

Figure 1. HIGS mechanism. The transgenic plant produces paperclip (pc)RNA or double-stranded (ds)RNA complementary to a target mRNA in the pathogen. The ds/pcRNA progresses through the RNAi pathway. The RNA-induced silencing complex (RISC) binds to the target mRNA in the pathogen and cuts it, silencing the protein(s) it codes for. Adapted from Ghag (2017), created with BioRender.com.

This process effectively slows the ability of the pathogen to infect the plant (Maximiano *et al.* 2022). Unlike broad-spectrum fungicides, the siRNA in HIGS is specific to a fungal species, allowing beneficial fungi to remain unharmed. The protection method is encoded into the DNA of the plant, making HIGS heritable and eliminating the need to reapply the protection method periodically as one would need to do with fungicides. These features allow HIGS to be more time and cost-effective as well as more eco-friendly.

A previous study using spray-induced gene silencing (SIGS), an exogenous RNAi method where a solution of RNA molecules and anti-degradation agents are applied externally to the plant, demonstrated that the *Sclerotinia* gene SS1G_07873 reduces Sclerotinia lesion size on canola leaves by 64% and *A. thaliana* leaves by 46% (McLoughlin *et al.* 2018). SS1G_07873

codes for 20S-pre-rRNA D-site endonuclease NOB1. SS1G_07873 is involved in processing the 20S-pre-rRNA into mature 18S rRNA in order to synthesize a functional 40S ribosomal subunit (https://string-db.org/cgi/network?taskId=b2637tYxcmyV&sessionId=bTE2CVqR5j7e) . The ribosome is required to synthesize proteins for the fungi, making SS1G_07873 an essential gene for growth and survival. Knocking down an essential protein for translation limits the amount of proteins formed by the fungus thus slowing its growth and rate of infection on the plant, allowing natural plant defenses to take effect. McLoughlin *et al.* 2018 demonstrated this effectiveness using a topical treatment, whereas I have translated this success in a transgenic model.

In addition to studying the knockdown of their target gene, SS1G_01703, Walker *et al.* (2023) also evaluated the impact of HIGS on non-target genes known to interact with SS1G_01703. They found that both the target gene and the interacting genes tested experienced decreases in relative transcript abundance. SS1G_07873 has known interacting partners, including SS1G_05100 (TSR1), a Bms1-type G domain-containing protein, SS1G_08606 (RIOK2), a RIO domain-containing protein, and SS1G_08823 (LTV1), a shuttle protein for nuclear export of the small ribosomal subunit, found through co-expression analyses (Kırlı *et al.* 2015; Schafer 2003; Seiser *et al.* 2006). Like SS1G_07873, all three genes indicated are involved in the biogenesis and maturation of the small ribosomal subunit. Therefore impacting the transcript abundance of SS1G_07873 may also affect the abundance of these interacting partners (Kırlı *et al.* 2015; Schafer 2003; Seiser *et al.* 2006).

Long dsRNAs (dsRNA) are primarily used in the expression vector of genetically engineered plants for HIGS (Koch *et al.* 2013; Qi *et al.* 2017). One issue with dsRNA is the open ends of the structure, which are vulnerable to nucleases (figure 2) (Abbasi *et al.* 2020).

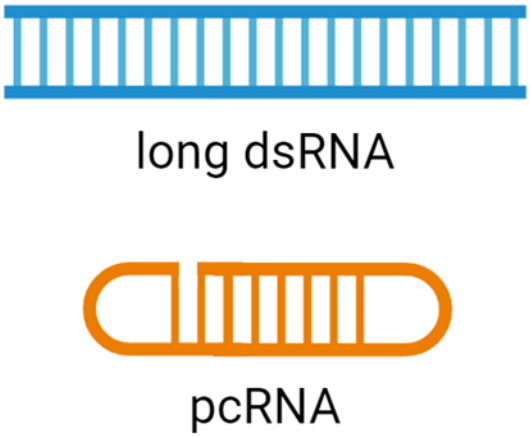

Figure 2. RNA interference (RNAi) structures. Top: long double-stranded RNA (long dsRNA) (blue). Bottom: paperclip RNA (pcRNA) (orange). Adapted from Abbasi *et al.* (2020), created with BioRender.com.

A novel way of solving this issue is to create an alternate structure that folds over itself on both ends but is not covalently annealed, protecting it from degradation and increasing its stability (Abbasi *et al.* 2020). This structure has been termed paperclip RNA (pcRNA) (figure 2). The pcRNA study on the mosquito *Aedes aegypti* found the uptake process differed from the typical clathrin-mediated uptake mechanism of dsRNA (Abbasi *et al.* 2020). A clathrin-independent uptake mechanism allows the possibility that pcRNA could be an effective RNAi method on organisms with differing or resistant uptake mechanisms (Abbasi *et al.* 2020). While the study with pcRNA was conducted on an insect model, I have tested this structure in *S. sclerotiorum*. This choice is based not only on the increased stability of the structure but also because, like insects, fungi typically take up dsRNAi products through clathrin-mediated endocytosis (Abbasi *et al.* 2020; Wytinck *et al.* 2020).

Through my research, I have tested the effect of double-stranded and paperclip structures of SS1G_07873 against *S. sclerotiorium* using transgenic *Arabidopsis thaliana* lines. To do this, I have measured the lesion size on infected leaves, the knockdown of the *Sclerotinia* target genes,

and the knockdown of genes known to interact with SS1G_07873. If this work proves successful, it provides further evidence that HIGS can be used as a strategy to create canola varieties that are resistant to *S. sclerotiorum* and added to existing transgenic crops to further increase resistance in order to lessen our dependence on broad-spectrum fungicides.

Research objective: The objective of my honours project thesis is to demonstrate the effectiveness of HIGS using ds and pcRNA in reducing disease caused by *Sclerotinia sclerotiorum* in the model plant *Arabidopsis thaliana* to better understand HIGS as a tool to protect plants against fungal pathogens.

Hypotheses:

1. *A. thaliana* genetically engineered to produce RNAs coding for the *Sclerotinia* gene SS1G_07873 will present lower rates of disease compared to wild-type plants when inoculated with *S. sclerotiorum*.
2. *A. thaliana* genetically engineered to produce pcRNAs coding for *Sclerotinia* genes will present lower rates of disease compared to those engineered to produce dsRNAs when inoculated with *S. sclerotiorum*.

Methods and Materials

Plant material

Transgenic *Arabidopsis thaliana* expressing either pc or dsRNA SS1G_07873 in the T2 and T3 generation were used. These plants were developed before the start of my honours thesis. Briefly, transgenic plants were developed using the *Agrobacterium*-mediated spray transformation method described in Walker *et al.* (2023). These plants carry a kanamycin resistance insertion plasmid along with dsRNA SS1G_07873 or pcRNA SS1G_07873 (see figures 3 and 4 for plasmid sequences).

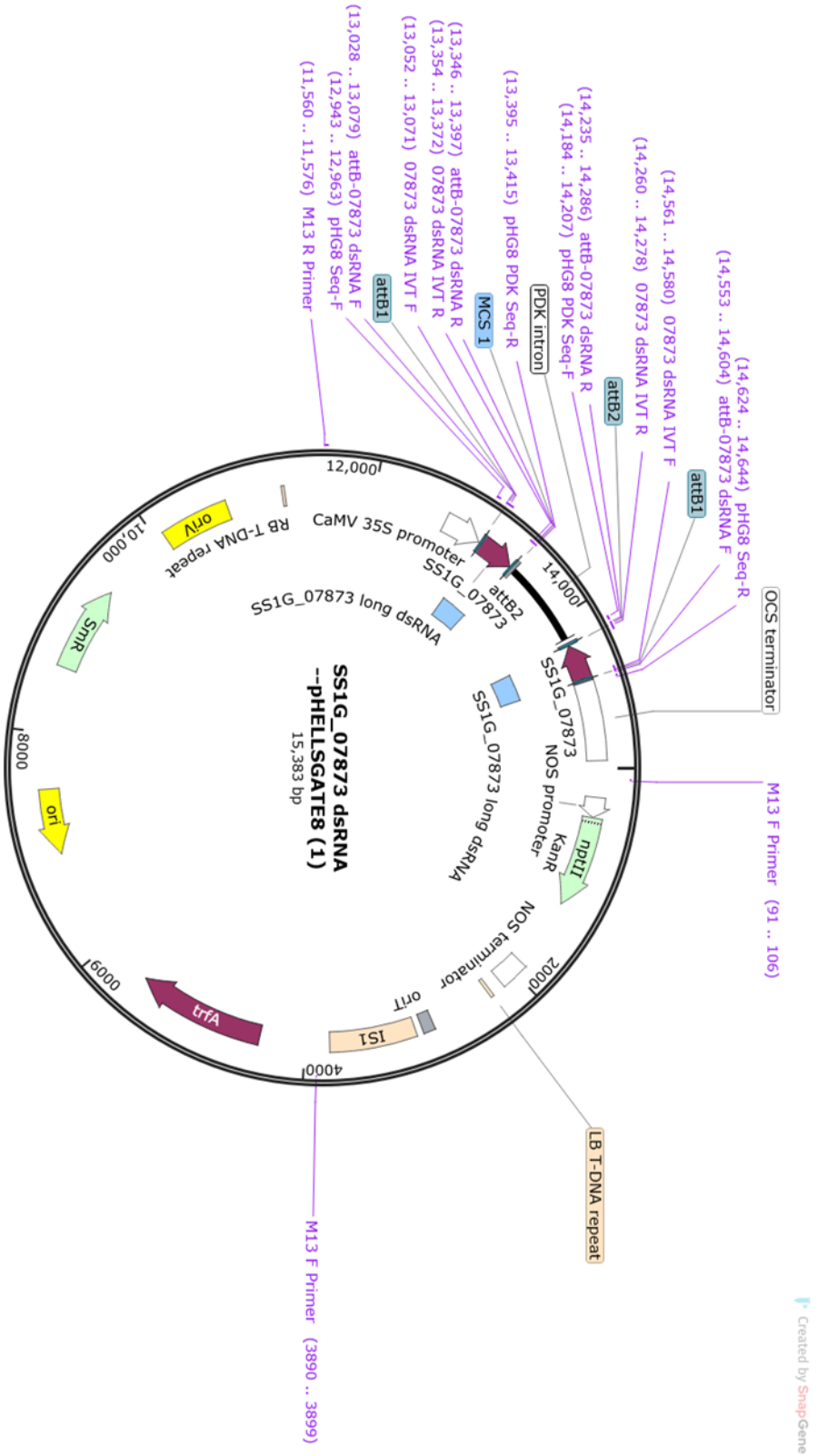

Figure 3. *Agrobacterium* plasmid gene map for SS1G_07873 double-stranded (ds)RNA. Created on Snapgene software (www.snapgene.com).

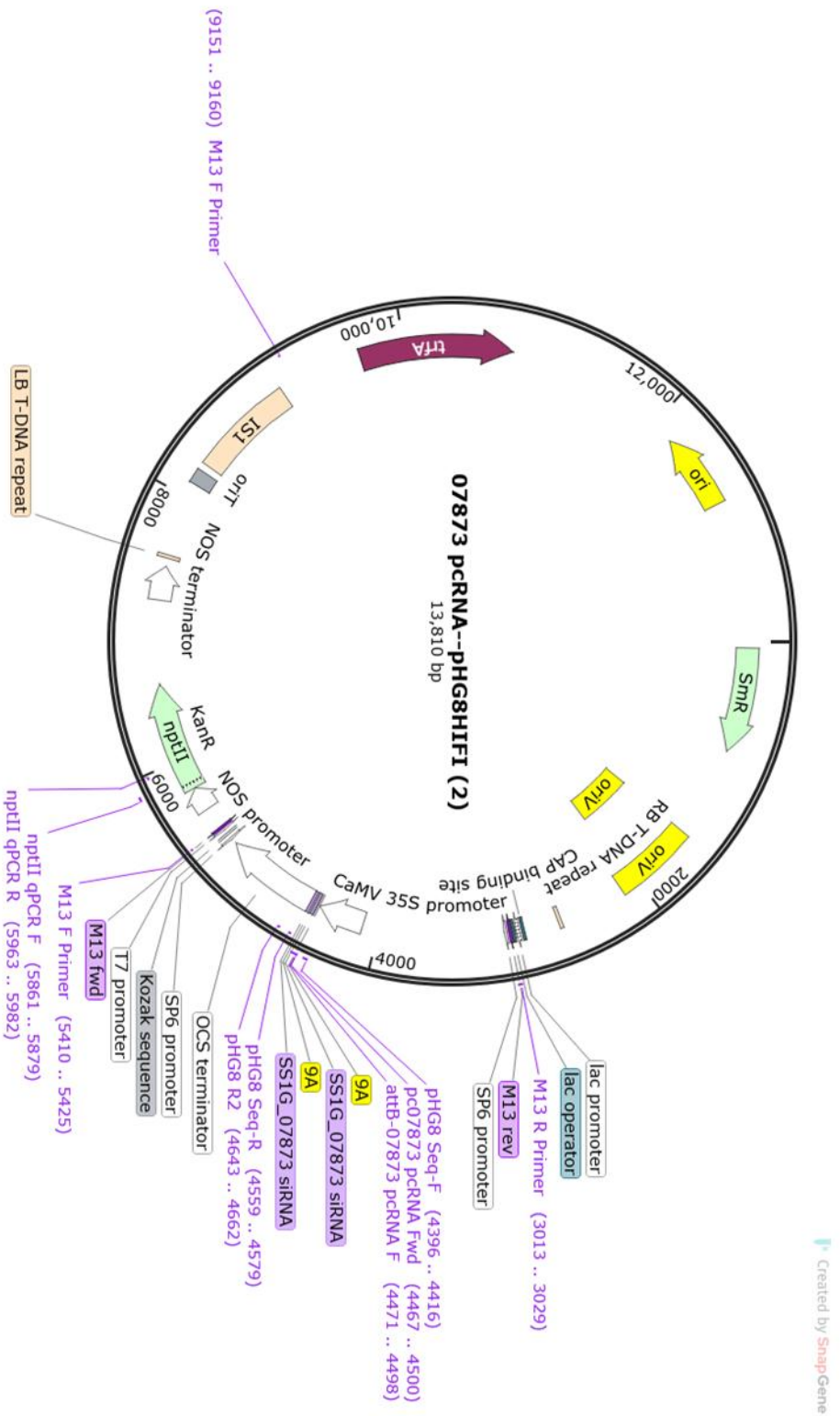

Figure 4. *Agrobacterium* plasmid gene map for SS1G_07873 paperclip (pc)RNA. Created on Snapgene software (www.snapgene.com).

Transgenic controls with gene inserts unrelated to *S. sclerotiorum* (dsRNA GUS and pcRNA GUS) were also developed in the lab before my arrival using the same methods as above. The resulting seeds are plated on kanamycin selection media (0.5 MS, 1µg/ml KAN, and agar), incubated in a growth chamber at 21˚C and 120µmol/m^2/s of light. After 2 weeks, seedlings are transplanted into 6-well trays and grown in a growth chamber at 21˚C and 120µmol/m^2/s of light. The resulting plants are of the T0 generation, each plant is the result of a unique insertion event and are labelled as separate "events". Seeds were collected from T0 plants and are plated on KAN selection media and transplanted flats containing Sungro® Professional soil mix. These T1 plants were sampled, and the DNA is extracted using the CTAB method as described in the following section. A Real-time qPCR was run on the DNA using primers selecting for the KAN resistance gene using methods described below in the *Quantifying knockdown of target and interacting genes in* S. sclerotiorum section. Results were used to determine the copy number of the transgene and plants are selected for homozygosity using the ΔΔCt method (Livak & Schmittgen 2001). Homozygous plants from each event will be raised to the T3 generation.

The *S. sclerotiorum* used is Acc2296 from Dr. Khalid Rashid (Agriculture and Agri-Food Canada) and is grown on ¼ strength potato dextrose agar plates with 50µg/ml tetracyclin and kept in a dark drawer at room temperature. Subcultures are made every three days using a 1mm plug from the growing edge of the *S. sclerotiorum* mycelia.

Detached leaf infection assay procedures

Round one assays were performed to evaluate which events to process for molecular analysis. Round one assays were performed by placing 24 leaves for each of six dsRNA and six pcRNA events (two leaves each from 12 plants) in the T2 generation as well as GUS transgenics and 72 wild-type (WT) leaves in a sealed transparent box with moist paper towels (figure 5).

Figure 5. Example of a detached leaf infection assay set-up. Round two pictured (20 leaves per event). WT rows are the first, fifth and last rows (20 leaves each, total: 60 leaves).

WT acts as a negative control and GUS as a transgenic negative control. WT leaves are separated into three rows: top, middle, and bottom of the box. This procedure seals in moisture and creates an optimal environment for *S. sclerotiorum* infection and the separation of WT leaves controls for variation within the box. Each leaf was inoculated with 10µl of Sclerotinia slurry (a ratio of 0.60g of the outer 1cm of fungal growth on three-day-old plates to 600µl of 0.1% agarose). The box was then incubated in a growth chamber at 21˚C and 10µmol/m^2/s of light for three days. After three days post-inoculation (dpi), images of the box were taken with a light board. Lesion areas were measured using ImageJ software (imagej.nih.gov) and the percent change in lesion size was calculated relative to WT using the formula: (median WT lesion area – median event X lesion area)/median WT lesion area x 100. The median was used to avoid skewed means caused by outliers. Leaves that are folded, overconsumed, or do not show any lesion were omitted. The top two performing events and one worst performing event for both dsRNA and pcRNA transgenic lines were selected for round two assays.

Round two assays were performed to collect data on lesion size as well as collect samples for molecular analysis. The assay process described above is repeated for round two assays using the selected events (two best and one worst-performing event for both ds and pcRNA transgenics), the GUS transgenics, and WT plants from the T3 generation due to limited seed stock in the T2 generation (figure 5). Round two assays were performed with 20 leaves per event (two leaves each from ten plants) and 60 WT leaves, with the GUS and WT plants acting as negative controls. Uninfected leaf samples were taken from each plant used for the assay at the time of inoculation. DNA and RNA were extracted to run a genotyping PCR (primers indicated in table 1). Leaves chosen for sampling were similarly sized to the assay leaves as to better represent the state of the assay leaves when infected. Images were taken and ten infected leaf samples from each event including GUS transgenics and WT plants were selected for further molecular analysis.

DNA and RNA extractions

DNA and RNA CTAB and lithium chloride extractions were completed for uninfected and infected samples following the protocol from Kiss *et al.* (2024). Ten leaf samples were taken from each event for extraction. Out of the ten samples, only samples within one standard deviation from the mean in terms of lesion size were extracted. All events had at least seven of the ten samples taken within the standard deviation. After extractions, nanodrop readings were performed to ensure sufficient yield and minimal contamination. RNA extracted from infected leaves using the CTAB and lithium chloride precipitation was used for *Quantifying knockdown of target genes and interacting genes in* S. sclerotiorum as described below.

Detection of dsRNA or pcRNA gene insert in A. thaliana

DNA from uninfected samples was used to run a genotyping PCR to ensure round two assay plants contain the correct transgene. A PCR was used to amplify the transgene (using primers and conditions indicated in table 1, designed using the Integrated DNA Technologies' (IDT) PrimerQuest Tool (https://www.idtdna.com/Primerquest/Home/Index)) and run on a 1.5% agarose gel at 350 volts along with the SS1G_07873 plasmid, no template control (NTC), and WT.

Quantifying knockdown of target and interacting genes in S. sclerotiorum

Extracted RNA from infected leaves was used to perform a Reverse-transcriptase PCR to measure the amount of target mRNA present in the *S. sclerotiorum.* cDNA was synthesized as described in McLoughlin *et al.* (2018), using Maxima First Strand reverse transcriptase (Thermo Scientific, Waltham, MA, US) using 500 ng of RNA in a 10 µL reaction. Using the synthesized cDNA, transcript levels for the target gene SS1G_07873 were measured as described in McLoughlin *et al.* (2018), by running a Real-time qPCR on the Bio-Rad CFX96 Connect Real-Time system using SsoFast EvaGreen Supermix (Bio-Rad Laboratories, Hercules, CA, US) in 15 µL reactions according to the manufacturer's protocol and using primers designed using the IDT PrimerQuest Tool (https://www.idtdna.com/Primerquest/Home/Index) (primers indicated in table 2). Four samples were measured for each event including WT and the transgenic controls. The samples used were selected based on high yield, minimal contamination, and similarity in lesion size to the median. Experimental triplicates were performed for the qPCR along with a NTC and -RT control. Relative accumulation was calculated using the ΔΔCt method, normalized to Sac7 (SS1G_12350) and Sstub1 (SS1G_04652) and relative to the WT control (Livak & Schmittgen 2001; Llanos *et al.* 2015). The same method was used to measure the transcript

levels for three genes known to interact with SS1G_07873 including SS1G_05100 (TSR1), SS1G_08606 (RIOK2), and SS1G_08823 (LTV1) (Kırlı *et al.* 2015; Schafer 2003). GUS transgenic controls will not be tested to save time and reagents.

Entropy estimation of pcRNAs

The RNAfold web server from ViennaRNA Web Services (rna.tbi.univie.ac.at) was used to estimate the entropy of the 25-nucleotide section of SS1G_07873 used to create the transgenic plants. The FASTA sequence for SS1G_07873 from NCBI will be the input for the system. The coloured free energy prediction of the website for the input will then be compared with the pcRNA nucleotide section to estimate the entropy.

Statistical tests

To determine whether measured lesion size varies significantly, data will be subject to ANOVA and Pairwise T-tests (significance $p \geq 0.05$) and a Shapiro-Wilk test to ensure normality using RealStatistics software add-in on Microsoft Excel. A Dunn's test will be performed as opposed to Pairwise T-tests if the data does not follow a normal distribution. RT-qPCRs for quantifying *S. sclerotiorum* target and interacting genes will be performed in experimental triplicates and significance determined using unpaired, two-tailed T-tests ($p \geq 0.05$).

Results

Detached-leaf assays

Round 1 assays were completed with SS1G_07873 T2 transgenic *A. thaliana* with the following events: ds1, ds2, ds3, ds4, ds5, ds6, pc1, pc2, pc3, pc4, pc5, pc6. Percent difference in

lesion size relative to WT was calculated as well as the p-values (figure 6) 3 days post inoculation.

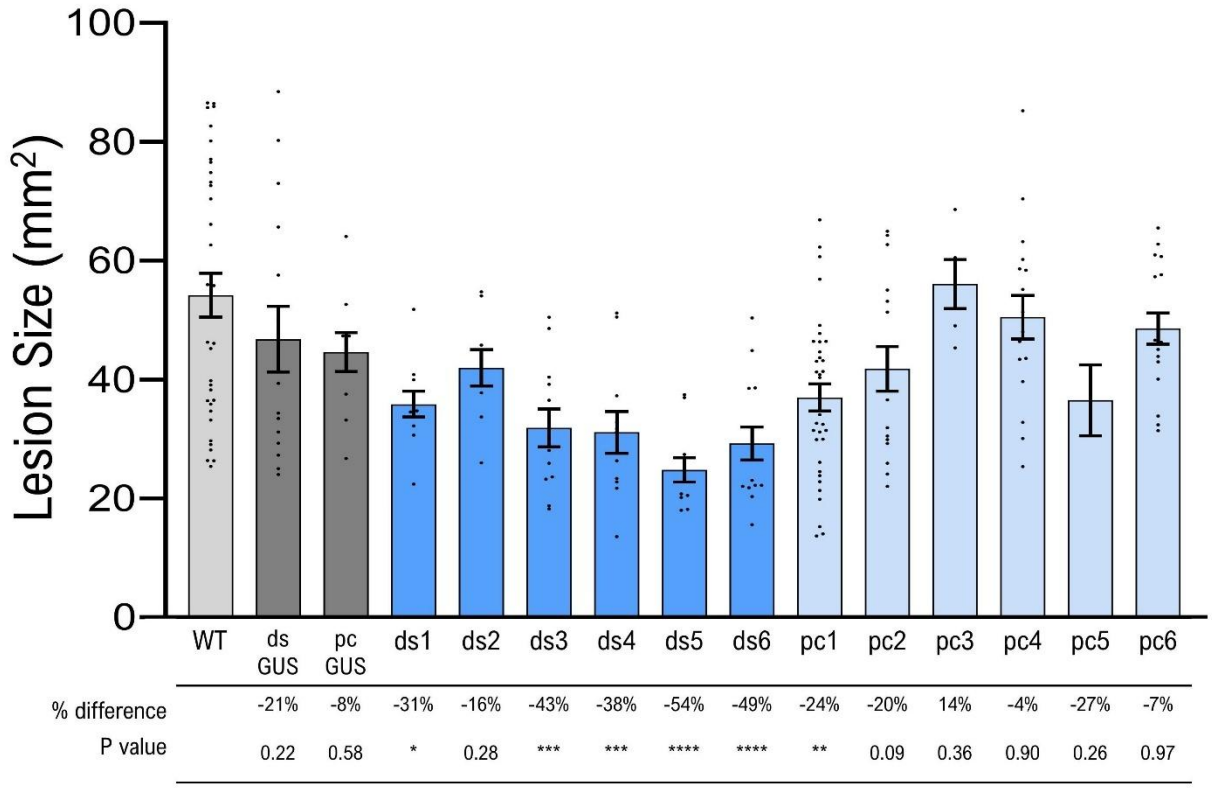

Figure 6. Lesion size in mm^2 of infected T2 07873 transgenic leaves three days post-inoculation (round one lesion assay). WT: wild type, ds: double stranded, pc: paperclip. Significance was calculated using a Dunn's test due to non-normality detected by a Shapiro-Wilk test. P-values: * <0.05, ** <0.01, ***<0.001, ****<0.0001.

Events ds1, ds3, ds4 ds5, ds6, and pc1 showed significant decreases in lesion size with ds5 having the largest decrease with a -54% difference compared to WT. All events, including the transgenic controls ds and pcGUS, demonstrated decreases in lesion size except pc3 which had a percent increase of 14%. Events ds5, ds6, pc1 and pc5 were selected for their improved protection against *S. sclerotiorum* while ds2 and pc3 were selected for their inability to slow lesion size. However, initial analysis on the round one assay were completed before the decision

to remove outliers via standard deviation had been made, therefore the events which were grown up in the T3 generation and used for round 2 assays were as follows: best performing (ds): ds3, ds5, best performing (pc): pc2, pc6, worst performing (ds): ds1, worst performing (pc): pc3.

Unfortunately, pc6 and pc3 plants showed signs of purpling and short roots of 0.5cm or less after the two-week incubation on the Kanamycin selection media. Seedlings either succumbed shortly after transplanting or matured slowly with deformed leaves making them unusable for the round 2 assay. Due to these complications, only four events were tested: ds3, ds5, ds1, and pc2 along with WT and the transgenic controls ds and pcGUS. The percent difference in lesion size relative to WT and the p-values were calculated (figure 7).

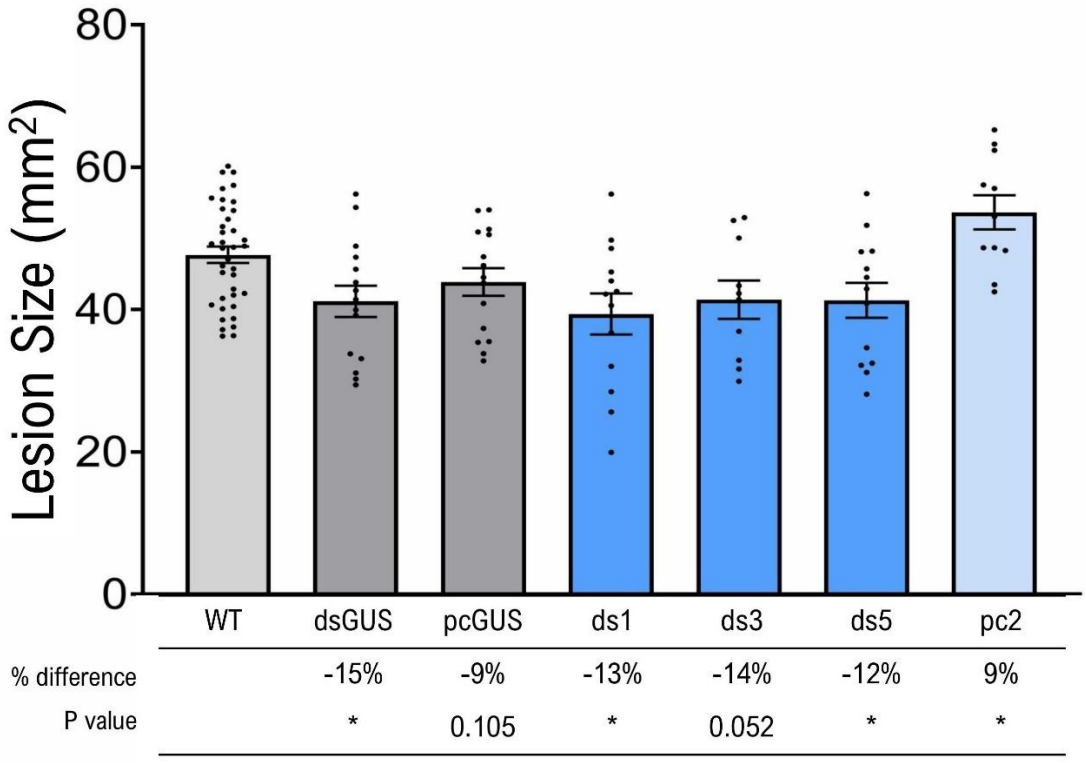

Figure 7. Lesion size in mm^2 of infected T3 07873 transgenic leaves three days post-inoculation (round two lesion assay). WT: wild type, ds: double stranded, pc: paperclip. Significance was calculated using Pairwise T-tests relative to WT. P-values: * <0.05.

Events ds1 and ds5 showed significant decreases in lesion size with a percent difference of -13% and -12% relative to WT, respectively. Event ds3 also demonstrated a difference in lesion size of -14% however, the result was insignificant with a p-value of 0.0522. Event pc2 showed a significant increase in lesion size with a percent difference of 9%. Interestingly, the transgenic controls saw decreases in lesion size with dsGUS showing a significant percent difference of -15%, outperforming all the SS1G_07873 transgenic events.

Detection of dsRNA or pcRNA gene insert in A. thaliana

Uninfected SS1G_07873 DNA samples were used to perform the genotyping PCR (primers and conditions in table 1) along with the SS1G_07873 plasmid, no template control (NTC), and WT (figure 8).

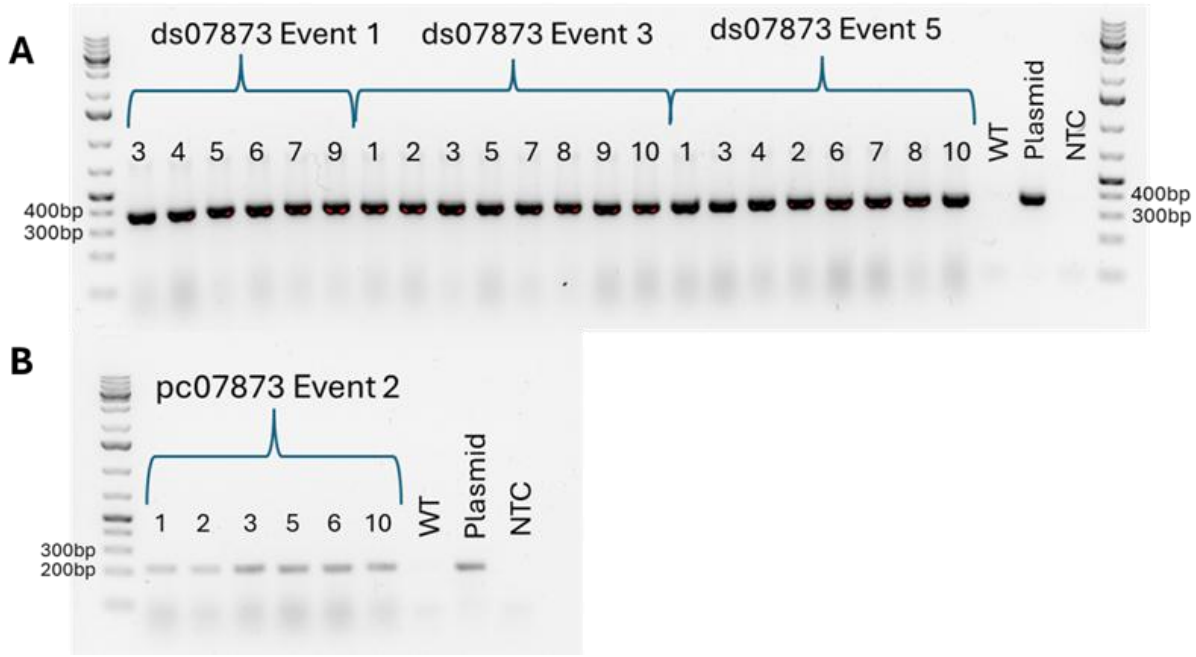

Figure 8. Genotyping PCR (primers and conditions in table 1) run on a 1.5% agarose gel at 350 volts for 35 mins. A. Double-stranded (ds) 07873 plants, wild-type (WT), SS1G_07873 ds plasmid, negative template control (NTC), and ladder (GeneRuler 1kb Plus DNA Ladder). Expected band size of 370bp, all plants positive for the transgene. B. Paperclip (pc) 07873 plants, WT, SS1G_07873 pc plasmid, NTC, and ladder. Expected band size of 221bp, all plants positive for the transgene.

A singular band was found at the expected location for all samples which matched the plasmid. Both WT and NTC resulted in no bands. This result confirms all plants used in the assay contain the transgene.

Quantifying knockdown of target and interacting genes in S. sclerotiorum

Though intended to be used as a second housekeeping gene to further validate results, Sstub1 was not used to normalize transcript abundance as an average decrease in relative abundance was observed in all transgenic SS1G_07873 genotypes with significant decreases in ds3, ds5, and pc2 when analyzed relative to Sac7 (figure 9).

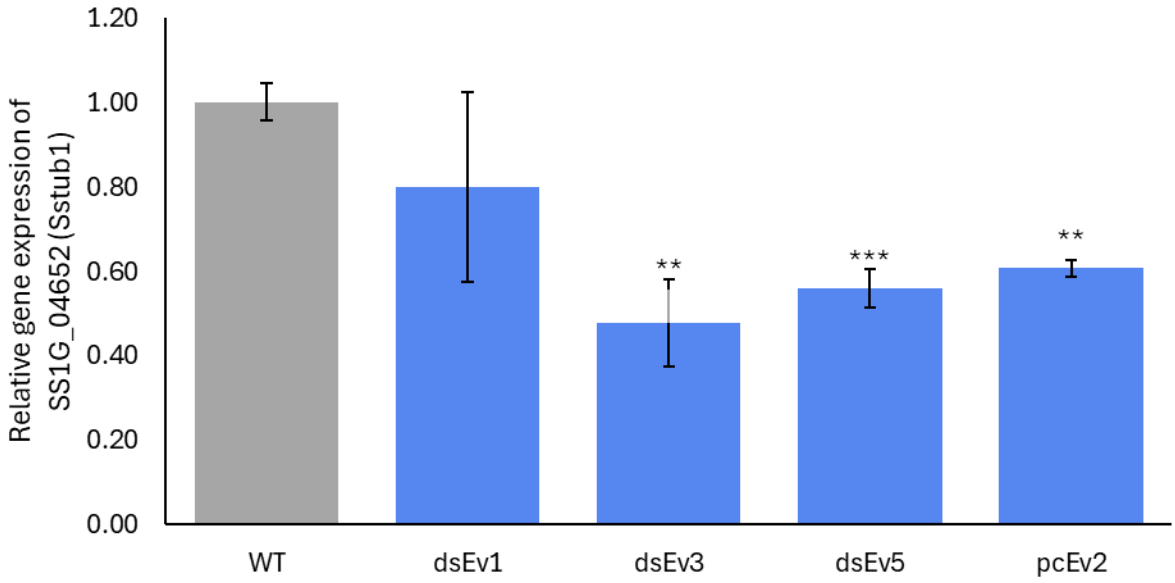

Figure 9. Relative gene expression of SS1G_04652 in *S. sclerotiorum* on infected leaves. Primer and conditions for qPCR in table 2. Normalized to SS1G_12350 (Sac7) expression and calculated with the ΔΔCt method relative to wild type (WT) (grey). ds: double stranded, pc: paperclip. Significance calculated using a two-tailed, unpaired T-test relative to WT. P-values: * <0.05, ** <0.01, ***<0.001.

Therefore, all genes will be measured relative to Sac7 with no additional housekeeping gene to verify results. There were inconsistent results in the relative transcript abundance of the target

gene, SS1G_07873. Ds1 and ds5 saw increases in transcript abundance, ds3 saw a decrease, and pc2 saw no change in transcript abundance compared to WT (figure 10).

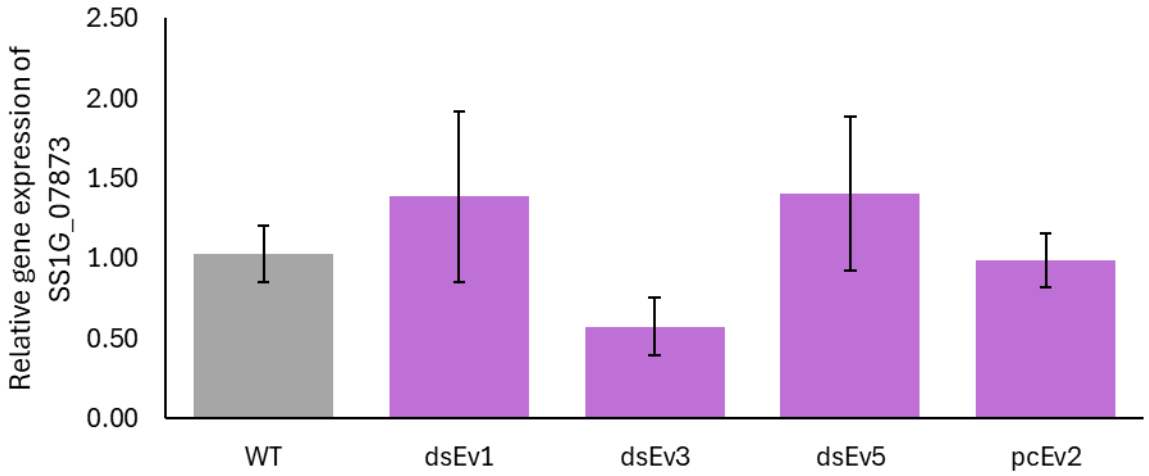

Figure 10. Relative gene expression of SS1G_07873 in *S. sclerotiorum* on infected leaves. Primer and conditions for qPCR in table 2. Normalized to SS1G_12350 (Sac7) expression and calculated with the ΔΔCt method relative to wild type (WT) (grey). ds: double stranded, pc: paperclip. No significance observed using a two-tailed, unpaired T-test relative to WT with an alpha of 0.05.

All changes in transcript abundance were not significant. The interacting genes SS1G_05100, SS1G_08606, and SS1G_08823 all experienced decreases in transcript abundance in all SS1G_07873 transgenic events. SS1G_05100 observed the largest decrease in transcript abundance with significant decreases in events ds3, ds5, and pc2 (figure 11).

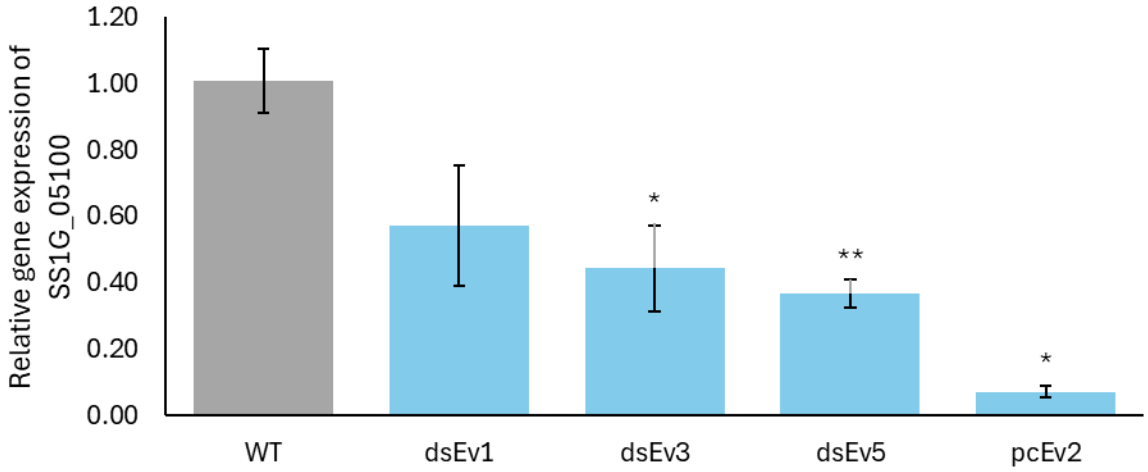

Figure 11. Relative gene expression of SS1G_05100 in *S. sclerotiorum* on infected leaves. Primer and conditions for qPCR in table 2. Normalized to SS1G_12350 (Sac7) expression and calculated with the ΔΔCt method relative to wild type (WT) (grey). ds: double stranded, pc: paperclip. Significance calculated using a two-tailed, unpaired T-test relative to WT. P-values: * <0.05, ** <0.01.

SS1G_08606 also experienced significant decreases in ds3, ds5, and pc2 (figure 12).

SS1G_08823 experienced a significant decrease in transcript abundance in pc2 and slight, insignificant decreases in all ds events (figure 13).

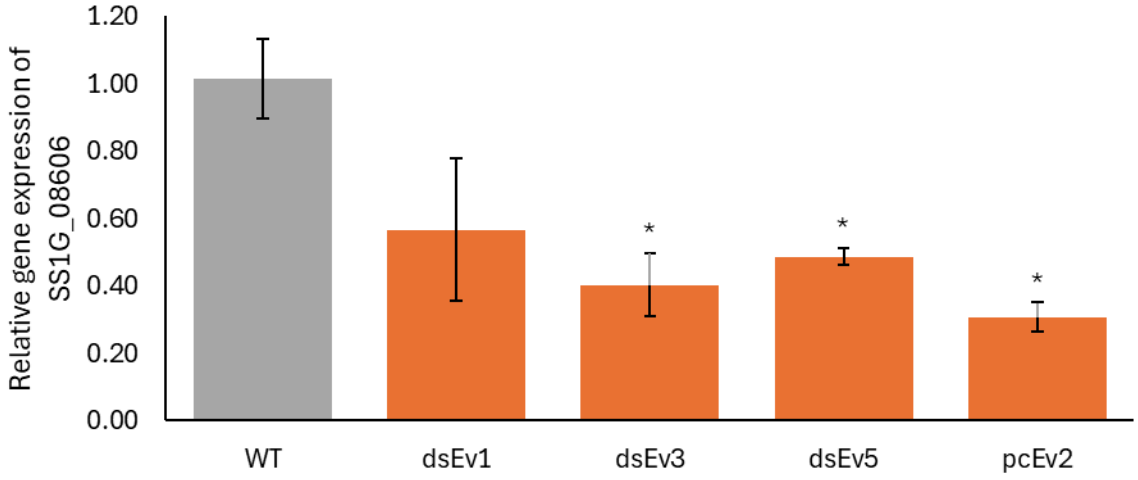

Figure 12. Relative gene expression of SS1G_08606 in *S. sclerotiorum* on infected leaves. Primer and conditions for qPCR in table 2. Normalized to SS1G_12350 (Sac7) expression and calculated with the ΔΔCt method relative to wild type (WT) (grey). ds: double stranded, pc: paperclip. Significance calculated using a two-tailed, unpaired T-test relative to WT. P-values: * <0.05.

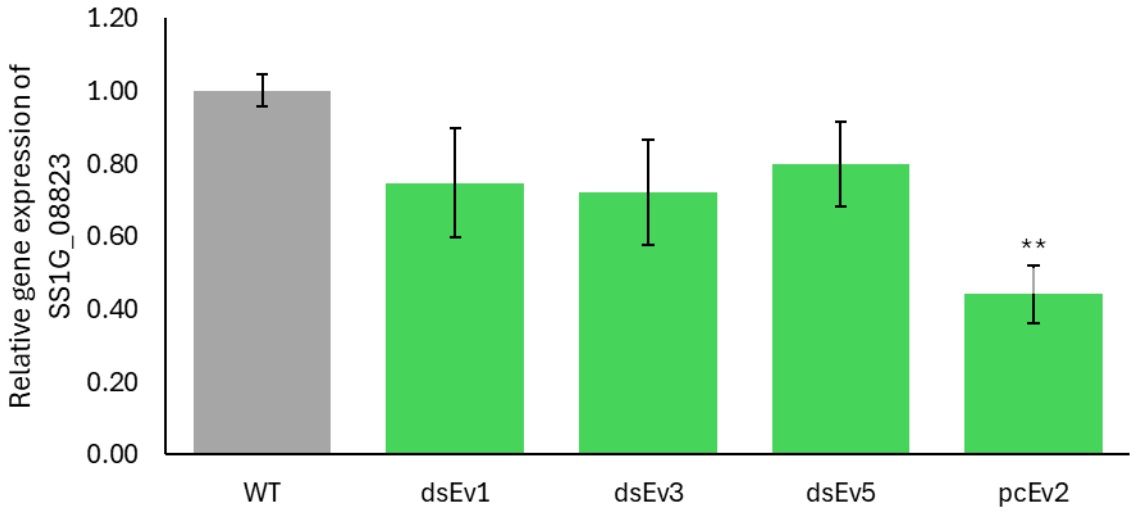

Figure 13. Relative gene expression of SS1G_08823 in *S. sclerotiorum* on infected leaves. Primer and conditions for qPCR in table 2. Normalized to SS1G_12350 (Sac7) expression and calculated with the ΔΔCt method relative to wild type (WT) (grey). ds: double stranded, pc: paperclip. Significance calculated using a two-tailed, unpaired T-test relative to WT. P-values: * <0.05, ** <0.01.

Entropy estimation of pcRNAs

Next, I predicted the fold structure of the SS1G_07873 mRNA sequence using the RNAfold web server from ViennaRNA Web Services (rna.tbi.univie.ac.at). The program generated two models, a minimum free energy (MFE) prediction and a thermodynamic ensemble (centroid) prediction (figure 14). Both models had comparable free energy folding requirements of -319.50 kcal/mol and -343.63 kcal/mol for the MFE and centroid predictions respectively. Both models also had similar positional entropy predictions for individual nucleotides. When compared with the pcRNA sequence, entropy predictions for the pcRNA can be made. Both models predicted the pcRNA sequence to have moderate entropy of an average positional entropy per base pair of 1.66 out of 3.6 (with 3.6 being the highest positional entropy possible). The MFE prediction placed the pcRNA sequence on a portion of a hairpin loop whereas the centroid prediction placed the sequence on the unpaired region of a large loop (figure 14).

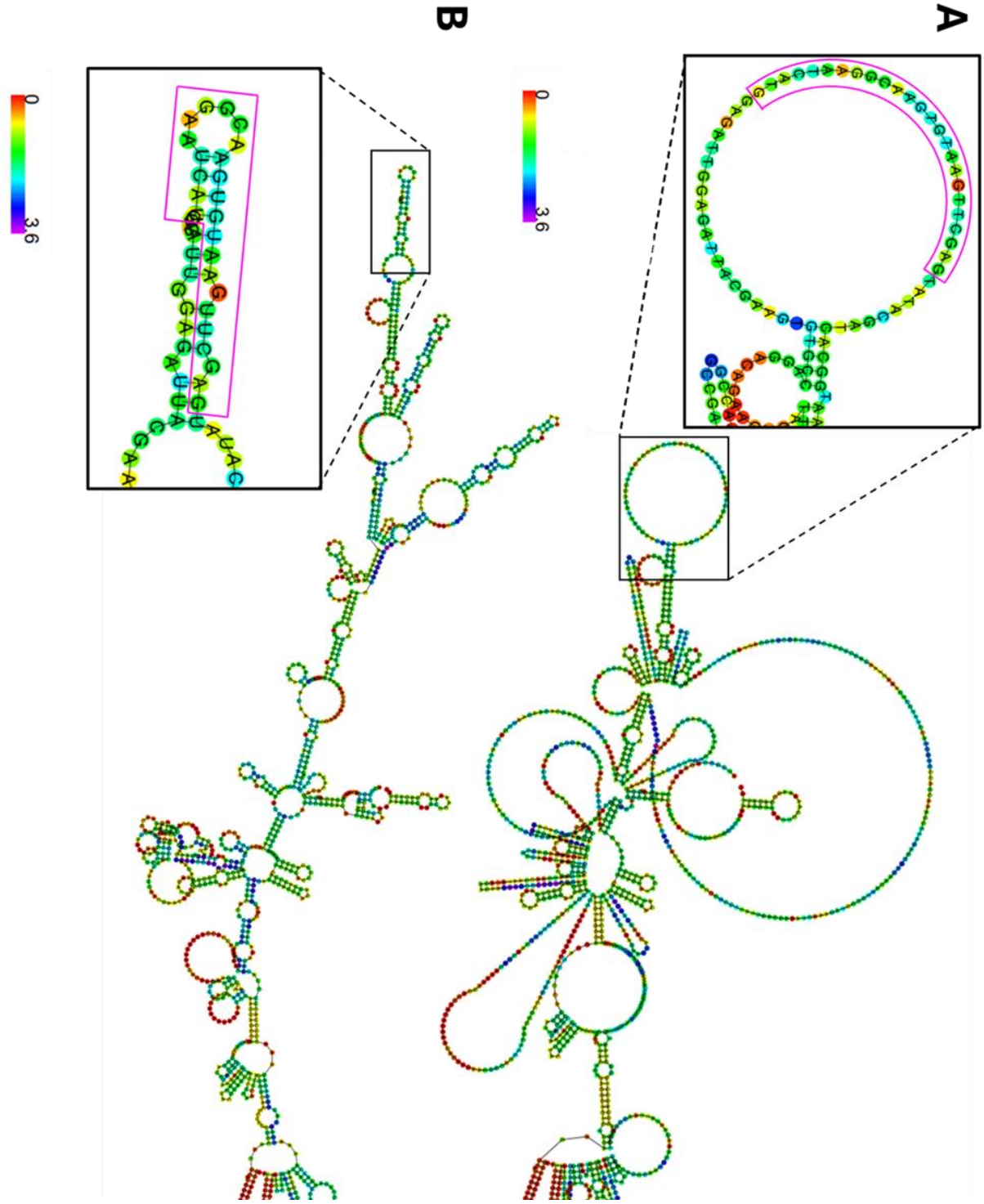

Figure 14. Minimum free energy (MFE) prediction (A) and a thermodynamic ensemble (centroid) prediction (B) models of SS1G_07873 mRNA. Close-up of the region where the pcRNA construct is generated from in the black box and circled in magenta. Each nucleotide is coloured based on its predicted entropy with red as the lowest and purple as the highest entropy. Generated using the RNAfold web server from ViennaRNA Web Services (rna.tbi.univie.ac.at).

Discussion

In previous research, topically applied SS1G_07873 RNA was found to be an effective gene target to reduce lesion size on plants and decrease SS1G_07873 transcript abundance in *S. sclerotiorum* (McLoughlin *et al.* 2018). This study aimed to build off those results and translate the success into a HIGS approach using transgenic *A. thaliana*.

Lesion analysis

The results of the round 2 assay demonstrated decreases in all ds events (ds1, ds3, ds5) with significant decreases for events 1 and 5. Event 3 is just shy of significance. This supports the idea that the siRNAs within the plant are affecting the growth of the *S. sclerotiorum* and slowing the infection, though the decreases in lesion size are not large, with percent differences of -13%, -14%, and -12% for ds1, ds3, and ds5 respectively. A previous SIGS study by McLoughlin *et al.* (2018) saw a greater decrease in lesion size when experimenting on *B. napus* as opposed to *A. thaliana.* Further experiments could include developing transgenic *B. napus* plants expressing ds SS1G_07873 which may also show a greater decrease in lesion size than the transgenic *A. thaliana* plants. The larger leaves of *B. napus* may allow for additional time for the RNAi system to act before the leaf gets overwhelmed. Due to this reason, SS1G_07873 should be investigated further for use in HIGS.

The event pc2 showed a significant increase in lesion size in the round 2 assay, contrary to the expectations due to paperclip structures being more stable than their double-stranded counterparts. This result may be due to the fact that the ds gene insert is much larger than the pc insert, allowing it to be cut by Dicer into several different siRNAs one or more of which may target an area on the mRNA with high entropy. Targeting areas with high entropy is optimal as they are more likely to be unpaired for easier binding to the siRNAs (Jia *et al.* 2012). Additionally, there may be a benefit to several RISC complexes holding different siRNAs

targeting an mRNA molecule as it may increase the likelihood of degradation. The entropy analysis on the pcRNA siRNA showed the target has a moderate entropy level, indicating there are siRNA options with higher entropies which may serve as better areas to target. To generate a more comparable analysis of the dsRNA and pcRNA transgenic plants, new pcRNA constructs should be developed while taking entropy scores into consideration. Additionally, studying how target gene mRNAs are diced should provide valuable information into RNAi design for future experiments.

Lesion size was reduced in the transgenic control plants expressing dsGUS. BLAST sequencing resulted in no matches with the *S. sclerotiorum* genome. Thus, GUS RNA should not be knocking down SS1G_07873 mRNA within the fungus. Additional experiments using transgenic plants expressing RNAs unrelated to *S. sclerotiorum* could be run to determine if they also show decreases in lesion size. The decrease in lesion size could be caused due to foreign RNA molecules within the plant generating an immune response. To test this theory, a qPCR using cDNA generated from RNA of uninfected GUS plants could be run to determine if immune response genes are expressed.

Earlier it was mentioned that the number of pc events in the round 2 assay decreased due to pc events 3 and 6 succumbing shortly after transplanting or being too deformed to use whereas those events were healthy in the previous round 1 assay. The sole difference in the assay plants was the generation. In round one, T2 plants were used, however, due to limited seed stock, the T2 progeny, T3, were used for the round two assay. Theoretically, the T2 and T3 plants from the same event should be genetically identical, as T1 plants were screened and confirmed homozygous. The SS1G_07873 insert uses a CaMV35S promoter whereas the KAN resistance gene uses a NOS promoter (figures 3 and 4). CaMV35S promoter is derived from the

Cauliflower Mosaic Virus, a natural plant pathogen which can infect *A. thaliana* in addition to many other plants (Schoelz & Shepherd 1988; Yu *et al.* 2003). Silencing or decreased expression of transgenes promoted by CaMV35S has been reported numerous times in various species (Rajeevkumar *et al.* 2015). This phenomenon may be triggered by RNA-directed DNA methylation (RdDM) of the promoter, resulting in silencing of the transgene (Matsunaga *et al.* 2019). Though this DNA methylation can occur at any generation, strong inhibition of the transgene is associated with the T3 generation and may provide evidence into my own results (Matsunaga *et al.* 2019). RdDM is most common when using CaMV35S promoter, however, it still occurs on the NOS promoter as well, therefore it is possible both the SS1G_07873 insert and KAN resistance gene were methylated (Cao 2003). Since both the KAN resistance gene and SS1G_07873 gene are located close together, another possibility is that the DNA methylation may have spread from the CaMV35S promoter to the NOS promoter, resulting in silencing both transgenes (Daxinger *et al.* 2008). DNA methylation resulting in the silencing of the KAN resistance gene would explain the poor growth of most T3 seedlings on KAN plates. The methylation of the SS1G_07873 gene would explain the smaller differences in lesion size compared to WT in the round two lesion assay (T3 plants) vs the round one lesion assay (T2 plants). To test this hypothesis, bisulfite sequencing of the plant DNA can be used to indicate any methylated cytosines in the transgene promoters.

Quantifying knockdown of target and interacting genes in S. sclerotiorum

Results from the target gene qPCR were unexpected. In past studies, a decrease in lesion size typically correlates to a decrease in transcript abundance (Wytinck *et al.* 2022). However, inconsistent results were found with increases in transcript abundance for ds1 and ds5 events, a decrease in abundance for ds3, and no change in abundance for pc2. These results do not

correlate with the lesion sizes. Increases in transcript abundance were also found by Pant & Kaur (2024) though a hypothetical reason for the increases was not provided. A possible explanation could be that the fungus is upregulating the SS1G_07873 gene in order to compensate for the mRNA lost due to the targeted degradation.

Another explanation is investigating the Dicer-like protein responsible for processing the foreign RNA in the plant. Bakhat *et al.* (2025) found most siRNAs processed by the plant in a SIGS study were 22nt in length, characteristic of siRNAs produced by DCL2. While DCL2 is efficient at translational repression due to binding the mRNA transcript, it often does not cleave the transcript (Wu *et al.* 2020). If DCL2 is indeed the major Dicer responsible for processing the foreign RNA in HIGS, it would explain the insignificant results in SS1G_07873 mRNA levels despite a decrease in lesion size being observed, as the mRNA bound by RISC would be freed during RNA extraction and be amplified during the PCR process, even though it was translationally repressed.

Small RNA sequencing can be used to better understand how RNAs are processed in the fungus and plant. These experiments should provide insight into how Dicer processes foreign RNA in the plant, what siRNAs are present, and the quantity of siRNAs present. Results from these experiments will enhance our understanding of HIGS as well as provide insight into solutions for improved vector design and crop protection outcomes.

SS1G_05100, SS1G_08606, and SS1G_08823 interact closely with SS1G_07873, therefore, it would be expected for transcript abundance trends of the interacting genes to match that of SS1G_07873 (Kırlı *et al.* 2015; Schafer 2003). However, this was not the case. SS1G_05100 and SS1G_08606 saw significant decreases in ds3, ds5, and pc2, while SS1G_08823 saw a significant decrease in pc2. This differs from the insignificant results for the

transcript abundance of SS1G_07873. These results align with the previous hypothesis of DCL2 being involved in the processing of RNAs, as if there is repression of translation of SS1G_07873, there would be a decrease in transcripts for interacting genes. Though the three additional genes selected for testing are known to interact closely with SS1G_07873, the decrease in transcripts may be more indirect. SS1G_07873 is involved in ribosome biogenesis, therefore, any decrease in SS1G_07873 translation would affect ribosome quantity and thus, any protein synthesis in the fungus. The synthesis of transcription factors may be impacted and thus decrease the transcription of many genes, including the interacting genes evaluated. To test this, transcripts for several other genes unrelated to ribosome biogenesis as well as genes involved in coding for transcription factors should be evaluated for any knockdown effects.

Sstub1 (SS1G_04652) was originally tested with the purpose of being an additional reference gene along with Sac7 as it is considered a housekeeping gene and commonly used in HIGS *S. sclerotiorum* studies (Ding *et al.* 2021; Wu *et al.* 2022). However, transcript levels of Sstub1 between *S. sclerotiorum* on WT and transgenic leaves differed, and when calculated relative to Sac7, the ΔΔCt values indicated a significant decrease in transcript abundance in events ds3, ds5, and pc2. This result indicates that Sstub1 levels are affected by the transgenic plants relative to Sac7 despite Sstub1 is not being directly associated with ribosome biogenesis. The reduction in transcript abundance may be attributed to a decrease in the synthesis of transcription factors needed for its transcription. Sstub1 codes for beta-tubulin, which is part of the cytoskeletal structure (Takeshita *et al.* 2014). Beta-tubulin is also a component in microtubules, which are necessary for cell division and hyphal growth (Ovechkina *et al.* 2003; Takeshita *et al.* 2014). A reduction in lesion size on the assay leaves indicates slower growth of the fungus and therefore, less frequent cell divisions. This decrease in mitotic activity may result

in less Sstub1 being transcribed, as without cell division, there is less need for spindle fibres. In this way, the decrease in Sstub1 transcript abundance may be due to the suppressed growth of the *S. sclerotiorum.* To test this, Sstub1 transcript levels could be measured in other conditions where cell division is slowed such as in cooler temperatures to see if the discrepancies remain.

Some studies have theorized the potential for gene stacking, where siRNAs for multiple gene targets are expressed in the plant at once (Beernink *et al.* 2024; Storer *et al.* 2012). Koch *et al.* (2013) saw success with targeting three different CYP51 genes, involved in ergosterol biosynthesis. Gene stacking SS1G_07873 with one or more of the interacting genes I investigated could have synergistic effects on the decrease in lesion size.

In conclusion, while a decrease in lesion size among transgenic plants was observed, supporting my hypothesis, complications with the T3 generation plant growth and performance as well as the inconsistent SS1G_07873 transcript abundance and decreases in transcript abundance for SS1G_05100, SS1G_08606, SS1G_08823, and SS1G_04652 complicated these findings as they varied from other HIGS studies (Walker *et al.* 2023; Wytinck *et al.* 2022). Further experiments are required if SS1G_07873 is to continue to be considered for incorporation into crop plants as a fungal protection measure. With more research, HIGS using SS1G_07873 may serve to be a valuable tool to combat fungal pathogens affecting Canadian crops.

Literature Cited

Abbasi, R., Heschuk, D., Kim, B., & Whyard, S. (2020). A novel paperclip double-stranded RNA structure demonstrates clathrin-independent uptake in the mosquito *Aedes aegypti*. *Insect Biochemistry and Molecular Biology, 127*, 103492. https://doi.org/10.1016/j.ibmb.2020.103492

Andrade, C. M., Tinoco, M. L., Rieth, A. F., Maia, F. C., & Aragão, F. J. (2015). Host-induced gene silencing in the necrotrophic fungal pathogen *Sclerotinia sclerotiorum*. *Plant Pathology*, *65*(4), 626–632. https://doi.org/10.1111/ppa.12447

Bakhat, N., Jiménez-Sánchez, A., Ruiz-Jiménez, L., Padilla-Roji, I., Velasco, L., Pérez-García, A., & Fernández-Ortuño, D. (2025). Fungal effector genes involved in the suppression of chitin signaling as novel targets for the control of powdery mildew disease via a nontransgenic RNA interference approach. *Pest Management Science*. https://doi.org/10.1002/ps.8660

Beernink, B. M., Amanat, N., Li, V. H., Manchur, C. L., Whyard, S., & Belmonte, M. F. (2024). SIGS vs. HIGS: opportunities and challenges of RNAi pest and pathogen control strategies. *Canadian Journal of Plant Pathology*, *46*(6), 675–689. https://doi.org/10.1080/07060661.2024.2392610

Bernstein, E., Caudy, A. A., Hammond, S. M., & Hannon, G. J. (2001). Role for a bidentate ribonuclease in the initiation step of RNA interference. *Nature*, *409*(6818), 363–366. https://doi.org/10.1038/35053110

Boland, G. J., & Hall, R. (1994). Index of plant hosts of Sclerotinia sclerotiorum. *Canadian Journal of Plant Pathology*, *16*(2), 93–108. https://doi.org/10.1080/07060669409500766

Cai, L., Udayanga, D., Manamgoda, D. S., Maharachchikumbura, S. S. N., McKenzie, E. H. C., Guo, L. D., Liu, X. Z., Bahkali, A., & Hyde, K. D. (2011). The need to carry out re-inventory of plant pathogenic fungi. *Tropical Plant Pathology*, *36*(4), 205–213. https://doi.org/10.1590/s1982-56762011000400001

Cao, X. (2003). Role of the DRM and CMT3 methyltransferases in RNA-directed DNA methylation. *Current Biology*, *13*(24), 2212–2217. https://doi.org/10.1016/s0960-9822(03)00908-4

Daxinger, L., Kanno, T., Bucher, E., van der Winden, J., Naumann, U., Matzke, A. J., & Matzke, M. (2008). A stepwise pathway for biogenesis of 24-nt secondary siRNAs and spreading of DNA methylation. *The EMBO Journal*, *28*(1), 48–57. https://doi.org/10.1038/emboj.2008.260

Derbyshire, M. C., & Denton-Giles, M. (2016). The control of Sclerotinia stem rot on oilseed rape (*Brassica napus*): Current practices and future opportunities. *Plant Pathology*, *65*(6), 859–877. https://doi.org/10.1111/ppa.12517

Ding, Y., Chen, Y., Yan, B., Liao, H., Dong, M., Meng, X., Wan, H., & Qian, W. (2021). Host-induced gene silencing of a multifunction gene SSCND1 enhances plant resistance against *Sclerotinia sclerotiorum*. *Frontiers in Microbiology*, *12*. https://doi.org/10.3389/fmicb.2021.693334

Duan, Y.-B., Ge, C.-Y., & Zhou, M.-G. (2013). Molecular and biochemical characterization of *Sclerotinia sclerotiorum* laboratory mutants resistant to dicarboximide and phenylpyrrole fungicides. *Journal of Pest Science*, *87*(1), 221–230. https://doi.org/10.1007/s10340-013-0526-6

Dutton, M. V., & Evans, C. S. (1996). Oxalate production by fungi: Its role in pathogenicity and ecology in the soil environment. *Canadian Journal of Microbiology*, *42*(9), 881–895. https://doi.org/10.1139/m96-114

Elmhirst, J. (2023). Canadian Plant Disease Survey 2023 volume 103: Disease highlights 2022. *Canadian Journal of Plant Pathology*, *45*(sup1), 1–171. https://doi.org/10.1080/07060661.2023.2222486

Ghag, S. B. (2017). Host induced gene silencing, an emerging science to engineer crop resistance against harmful plant pathogens. *Physiological and Molecular Plant Pathology*, *100*, 242–254. https://doi.org/10.1016/j.pmpp.2017.10.003

Ghozlan, M. H., EL-Argawy, E., Tokgöz, S., Lakshman, D. K., & Mitra, A. (2020). Plant defense against necrotrophic pathogens. *American Journal of Plant Sciences*, *11*(12), 2122–2138. https://doi.org/10.4236/ajps.2020.1112149

Govrin, E. M., & Levine, A. (2000). The hypersensitive response facilitates plant infection by the necrotrophic pathogen botrytis cinerea. *Current Biology*, *10*(13), 751–757. https://doi.org/10.1016/s0960-9822(00)00560-1

Hammond, S. M., Bernstein, E., Beach, D., & Hannon, G. J. (2000). An RNA-directed nuclease mediates post-transcriptional gene silencing in *Drosophila* cells. *Nature*, *404*(6775), 293–296. https://doi.org/10.1038/35005107

Hammond, S. M., Boettcher, S., Caudy, A. A., Kobayashi, R., & Hannon, G. J. (2001). Argonaute2, a link between genetic and biochemical analyses of RNAi. *Science*, *293*(5532), 1146–1150. https://doi.org/10.1126/science.1064023

Jia, X. G., Han, Q. H., Feng, W., & Lu, Z. H. (2012). Selecting highly effective siRNAs by their modified entropies with mini-clusters. *Theoretical and Applied Fracture Mechanics*, *58*(1), 51–54. https://doi.org/10.1016/j.tafmec.2012.02.007

Kabbage, M., Williams, B., & Dickman, M. B. (2013). Cell death control: The interplay of apoptosis and autophagy in the pathogenicity of Sclerotinia sclerotiorum. *PLoS Pathogens*, *9*(4). https://doi.org/10.1371/journal.ppat.1003287

Kırlı, K., Karaca, S., Dehne, H. J., Samwer, M., Pan, K. T., Lenz, C., Urlaub, H., & Görlich, D. (2015). A deep proteomics perspective on CRM1-mediated nuclear export and nucleocytoplasmic partitioning. *eLife, 4*. https://doi.org/10.7554/elife.11466

Kiss, T., Karácsony, Z., Gomba-Tóth, A., Szabadi, K. L., Spitzmüller, Z., Hegyi-Kaló, J., Cels, T., Otto, M., Golen, R., Hegyi, Á. I., Geml, J., & Váczy, K. Z. (2024). A modified CTAB method for the extraction of high-quality RNA from mono-and dicotyledonous plants rich in secondary metabolites. *Plant Methods*, *20*(1). https://doi.org/10.1186/s13007-024-01198-z

Koch, A., Kumar, N., Weber, L., Keller, H., Imani, J., & Kogel, K.-H. (2013). Host-induced gene silencing of cytochrome P450 lanosterol C14A-demethylase–encoding genes confers strong resistance to *Fusarium* species. *Proceedings of the National Academy of Sciences*, *110*(48), 19324–19329. https://doi.org/10.1073/pnas.1306373110

Liu, J., Carmell, M. A., Rivas, F. V., Marsden, C. G., Thomson, J. M., Song, J.-J., Hammond, S. M., Joshua-Tor, L., & Hannon, G. J. (2004). Argonaute2 is the catalytic engine of mammalian RNAi. *Science*, *305*(5689), 1437–1441. https://doi.org/10.1126/science.1102513

Livak, K. J., & Schmittgen, T. D. (2001). Analysis of relative gene expression data using real-time quantitative PCR and the 2−ΔΔCT method. Methods, 25(4), 402–408. https://doi.org/10.1006/meth.2001.1262

Llanos, A., François, J. M., & Parrou, J.-L. (2015). Tracking the best reference genes for RT-qPCR data normalization in filamentous fungi. *BMC Genomics*, *16*(1). https://doi.org/10.1186/s12864-015-1224-y

LLC, G. B. (n.d.). *Software for Everyday Molecular Biology*. SnapGene. http://www.snapgene.com/

MacLeod, A., Pautasso, M., Jeger, M. J., & Haines-Young, R. (2010). Evolution of the international regulation of plant pests and challenges for future Plant Health. *Food Security*, *2*(1), 49–70. https://doi.org/10.1007/s12571-010-0054-7

Matsunaga, W., Shimura, H., Shirakawa, S., Isoda, R., Inukai, T., Matsumura, T., & Masuta, C. (2019). Transcriptional silencing of 35s driven-transgene is differentially determined depending on promoter methylation heterogeneity at specific cytosines in both plus- and minus-sense strands. *BMC Plant Biology*, *19*(1). https://doi.org/10.1186/s12870-019-1628-y

Maximiano, M. R., Santos, L. S., Santos, C., Aragão, F. J. L., Dias, S. C., Franco, O. L., & Mehta, A. (2022). Host induced gene silencing of *Sclerotinia sclerotiorum* effector genes for the control of White Mold. *Biocatalysis and Agricultural Biotechnology*, *40*, 102302. https://doi.org/10.1016/j.bcab.2022.102302

McLoughlin, A. G., Wytinck, N., Walker, P. L., Girard, I. J., Rashid, K. Y., de Kievit, T., Fernando, W. G., Whyard, S., & Belmonte, M. F. (2018). Identification and application of exogenous dsRNA confers plant protection against *Sclerotinia sclerotiorum* and *Botrytis cinerea*. *Scientific Reports*, *8*(1). https://doi.org/10.1038/s41598-018-25434-4

Mur, L. A., Kenton, P., Lloyd, A. J., Ougham, H., & Prats, E. (2007). The hypersensitive response; the centenary is upon us but how much do we know? *Journal of Experimental Botany*, *59*(3), 501–520. https://doi.org/10.1093/jxb/erm239

Nowara, D., Gay, A., Lacomme, C., Shaw, J., Ridout, C., Douchkov, D., Hensel, G., Kumlehn, J., & Schweizer, P. (2010). HIGS: Host-induced gene silencing in the obligate biotrophic fungal pathogen *Blumeria graminis*. *The Plant Cell*, *22*(9), 3130–3141. https://doi.org/10.1105/tpc.110.077040

Ovechkina, Y., Maddox, P., Oakley, C. E., Xiang, X., Osmani, S. A., Salmon, E. D., & Oakley, B. R. (2003). Spindle formation in *Aspergillus*is coupled to tubulin movement into the nucleus. *Molecular Biology of the Cell*, *14*(5), 2192–2200. https://doi.org/10.1091/mbc.e02-10-0641

Pant, P., & Kaur, J. (2024). Control of *Sclerotinia sclerotiorum* via an RNA interference (RNAi)-mediated targeting of SSPAC1 and SSSMK1. *Planta*, *259*(6). https://doi.org/10.1007/s00425-024-04430-1

PrimerQuest - design qPCR assays: IDT. Integrated DNA Technologies. (n.d.). https://www.idtdna.com/Primerquest/Home/Index

Qi, T., Zhu, X., Tan, C., Liu, P., Guo, J., Kang, Z., & Guo, J. (2017). Host-induced gene silencing of an important pathogenicity factor *PsCPK1* in *Puccinia striiformis* f. sp. *tritici* enhances resistance of wheat to stripe rust. *Plant Biotechnology Journal*, *16*(3), 797–807. https://doi.org/10.1111/pbi.12829

Rajeevkumar, S., Anunanthini, P., & Sathishkumar, R. (2015). Epigenetic silencing in transgenic plants. *Frontiers in Plant Science*, *6*. https://doi.org/10.3389/fpls.2015.00693

Riou, C., Freyssinet, G., & Fevre, M. (1991). Production of cell wall-degrading enzymes by the phytopathogenic fungus *Sclerotinia sclerotiorum*. *Applied and Environmental Microbiology*, *57*(5), 1478–1484. https://doi.org/10.1128/aem.57.5.1478-1484.1991

Schafer, T. (2003). The path from nucleolar 90s to cytoplasmic 40s pre-ribosomes. *The EMBO Journal*, *22*(6), 1370–1380. https://doi.org/10.1093/emboj/cdg121

Schoelz, J. E., & Shepherd, R. J. (1988). Host range control of cauliflower mosaic virus. *Virology*, *162*(1), 30–37. https://doi.org/10.1016/0042-6822(88)90391-1

Seiser, R. M., Sundberg, A. E., Wollam, B. J., Zobel-Thropp, P., Baldwin, K., Spector, M. D., & Lycan, D. E. (2006). LTV1 is required for efficient nuclear export of the ribosomal small

subunit in *Saccharomyces cerevisiae*. *Genetics*, *174*(2), 679–691. https://doi.org/10.1534/genetics.106.062117

Storer, N. P., Thompson, G. D., & Head, G. P. (2012). Application of pyramided traits against Lepidoptera in insect resistance management for *Bt* crops. *GM Crops & Food*, *3*(3), 154–162. https://doi.org/10.4161/gmcr.20945

SS1G_07873 protein (*Sclerotinia sclerotiorum*) - string interaction network. (n.d.). https://string-db.org/cgi/network?taskId=b2637tYxcmyV&sessionId=bTE2CVqR5j7e

Stukenbrock, E., & Gurr, S. (2023). Address the growing urgency of fungal disease in crops. *Nature*, *617*(7959), 31–34. https://doi.org/10.1038/d41586-023-01465-4

Takeshita, N., Manck, R., Grün, N., de Vega, S. H., & Fischer, R. (2014). Interdependence of the actin and the microtubule cytoskeleton during fungal growth. *Current Opinion in Microbiology*, *20*, 34–41. https://doi.org/10.1016/j.mib.2014.04.005

Walker, P. L., Ziegler, D. J., Giesbrecht, S., McLoughlin, A., Wan, J., Khan, D., Hoi, V., Whyard, S., & Belmonte, M. F. (2023). Control of white mold (*Sclerotinia sclerotiorum*) through plant-mediated RNA interference. *Scientific Reports*, *13*(1). https://doi.org/10.1038/s41598-023-33335-4

Wang, F., Huang, H.-Y., Huang, J., Singh, J., & Pikaard, C. S. (2023). Enzymatic reactions of AGO4 in RNA-directed DNA methylation: siRNA duplex loading, passenger strand elimination, target RNA slicing, and sliced target retention. *Genes & Development*, *37*(3–4), 103–118. https://doi.org/10.1101/gad.350240.122

Wang, Q., Mao, Y., Li, S., Li, T., Wang, J., Zhou, M., & Duan, Y. (2022). Molecular mechanism of *Sclerotinia sclerotiorum* resistance to succinate dehydrogenase inhibitor fungicides. *Journal of Agricultural and Food Chemistry*, *70*(23), 7039–7048. https://doi.org/10.1021/acs.jafc.2c02056

Williams, B., Kabbage, M., Kim, H.-J., Britt, R., & Dickman, M. B. (2011). Tipping the balance: *Sclerotinia sclerotiorum* secreted oxalic acid suppresses host defenses by manipulating the host Redox Environment. *PLoS Pathogens*, *7*(6). https://doi.org/10.1371/journal.ppat.1002107

Wu, H., Li, B., Iwakawa, H., Pan, Y., Tang, X., Ling-hu, Q., Liu, Y., Sheng, S., Feng, L., Zhang, H., Zhang, X., Tang, Z., Xia, X., Zhai, J., & Guo, H. (2020). Plant 22-nt siRNAs mediate translational repression and stress adaptation. *Nature*, *581*(7806), 89–93. https://doi.org/10.1038/s41586-020-2231-y

Wu, J., Yin, S., Lin, L., Liu, D., Ren, S., Zhang, W., Meng, W., Chen, P., Sun, Q., Fang, Y., Wei, C., & Wang, Y. (2022). Host-induced gene silencing of multiple pathogenic factors of *Sclerotinia sclerotiorum* confers resistance to sclerotinia rot in *Brassica napus*. *The Crop Journal*, *10*(3), 661–671. https://doi.org/10.1016/j.cj.2021.08.007

Wytinck, N., Sullivan, D. S., Biggar, K. T., Crisostomo, L., Pelka, P., Belmonte, M. F., & Whyard, S. (2020). Clathrin mediated endocytosis is involved in the uptake of exogenous double-stranded RNA in the white mold phytopathogen *Sclerotinia sclerotiorum*. *Scientific Reports*, *10*(1). https://doi.org/10.1038/s41598-020-69771-9

Wytinck, N., Ziegler, D. J., Walker, P. L., Sullivan, D. S., Biggar, K. T., Khan, D., Sakariyahu, S. K., Wilkins, O., Whyard, S., & Belmonte, M. F. (2022). Host induced gene silencing of the *Sclerotinia sclerotiorum* abhydrolase-3 gene reduces disease severity in *Brassica napus*. *PLOS ONE*, *17*(8). https://doi.org/10.1371/journal.pone.0261102

Yoder, J. A., Nelson, B. W., Jajack, A. J., & Sammataro, D. (2017). Fungi and the effects of fungicides on the honey bee colony. *Beekeeping – From Science to Practice*, 73–90. https://doi.org/10.1007/978-3-319-60637-8_5

Yu, W., Murfett, J., & Schoelz, J. E. (2003). Differential induction of symptoms in *Arabidopsis* by P6 of *cauliflower mosaic virus*. *Molecular Plant-Microbe Interactions*, *16*(1), 35–42. https://doi.org/10.1094/mpmi.2003.16.1.35

Zhang, X., & Fernando, W. G. (2018). Insights into fighting against blackleg disease of *Brassica napus* in Canada. *Crop and Pasture Science*, *69*(1), 40. https://doi.org/10.1071/cp16401

Zhou, F., Zhang, X.-L., Li, J.-L., & Zhu, F.-X. (2014). Dimethachlon resistance in *Sclerotinia sclerotiorum* in China. *Plant Disease*, *98*(9), 1221–1226. https://doi.org/10.1094/pdis-10-13-1072-re

Appendix

Table 1. Primers and cycle conditions for performing a genotyping PCR for transgenic *A. thaliana*. Forward (F) and reverse (R) primers for SS1G_07873 dsRNA and pcRNA plasmids. Primers designed using IDT PrimerQuest Tool.

Gene Target		Primer
Ss07873 dsRNA	F	ACGTGCAGCAAGTTTGTACAAAAAAGCAGGCTttcgaaaccaccctgctacctttcctca
	R	GTCAATAGCCACTTTGTACAAGAAAGCTGGGTcccatgcgcctctagtttcaatttttgg
Ss07873 pcRNA	F	ACGTGCAGCAAGTTTGTACAAAAAAGCAGGCTCATGTTTTTTTTTCATGATGAGCTTGAA
	R	AAACCGGCGGTAAGGATCTG
		Cycle conditions
Ss07873 dsRNA		35 cycles, 30 second melt, 30 second anneal (64C), 45 second extension
Ss07873 pcRNA		40 cycles, 30 second melt, 30 second anneal touchdown (70C -> 50C), 45 second extension

Table 2. Primers and cycle conditions for performing a transcript knockdown qPCR on cDNA from infected leaves. Forward (F) and reverse (R) primers for SS1G_07873, SS1G_05100, SS1G_08606, SS1G_08823, SS1G_04652 (Sstub1) (HKG) and SS1G_12350 (Sac7) (HKG). Primers designed using IDT PrimerQuest Tool.

Gene Target		Primer
Ss07873	F	AGAATGATCCCTCAGCCTCTAC
	R	GGCTCTTGTAACGGCATCTT
Ss05100	F	AGAGACGCACGGATGAAATG
	R	GGTACGTTGCGAAGGTGAATA
Ss08606	F	ACTCACAGCAGTCGAACAAG
	R	CTCGCAGAGCCGTCATAAAT
Ss08823	F	GACAAACCCTTCCGCTTACT
	R	CCTCGTCTAACTGTTCCATACC
Ss04652 (Sstub1)	F	GCTGCTTTCTGGCAAACTATC
	R	CTCACGACGAACGACATCAA
Ss12350 (Sac7)	F	CGATACTGTGCCTGTGACCA
	R	CCTCTCCTCAAGCGCCATAG
		Cycle conditions
		40 cycles, 30 sec enzyme activation, 5 sec denaturation, 5 sec annealing/extension, 5 sec melt curve (65C -> 95C)

Table 3. Nanodrop results for DNA and RNA extracted from infected *A. thaliana* leaves. Extracted using the CTAB and lithium chloride precipitation method as described in Kiss *et al.* (2024). Samples highlighted in yellow were selected for measuring transcript knockdown via RT-PCR and qPCR. ds: double stranded, pc: paperclip. For WT, T: top row, M: middle row, B: bottom row.

	Infected DNA			Infected RNA		
Sample Name	**Nucleic Acid(ng/uL)**	**A260/A280**	**A260/A230**	**Nucleic Acid(ng/uL)**	**A260/A280**	**A260/A230**
WT#T17	603.64	1.891	1.173	1659.646	2.139	2.48
WT#M2	517.744	1.923	1.32	1079.482	2.083	2.52
WT#M9	599.283	1.916	1.2	1737.163	2.147	2.476
WT#M12	386.216	1.956	1.423	1015.911	2.088	2.487
WT#M18	395.547	1.989	1.506	928.069	2.084	2.521
WT#B11	537.912	1.974	1.259	1228.293	2.111	2.504
WT#B13	530.32	1.869	1.232	1922.625	2.191	2.384
WT#B14	501.502	1.945	1.377	1263.645	2.114	2.516
WT#B16	397.394	2.017	1.527	848.285	2.098	2.55
dsGUS#3	512.397	1.901	1.224	1029.812	2.107	2.496
dsGUS#9	464.188	1.98	1.459	962.814	2.098	2.494
dsGUS#15	383.435	2.019	1.557	977.934	2.096	2.514
dsGUS#17	294.892	2.062	1.65	834.311	2.091	2.474
dsGUS#18	458.997	1.907	1.257	708.62	2.065	2.518
dsGUS#19	416.563	1.958	1.452	955.633	2.136	2.432
pcGUS#1	552.508	1.925	1.231	1654.064	2.168	2.38
pcGUS#3	315.053	2.039	1.631	1424.068	2.131	2.489
pcGUS#5	348.002	2.064	1.613	958.972	2.11	2.501
pcGUS#6	248.539	2.073	1.915	544.363	2.064	2.55
pcGUS#10	505.201	1.973	1.416	1011.181	2.119	2.456
pcGUS#13	344.11	2.087	1.644	753.866	2.066	2.518
pcGUS#14	324.836	2.028	1.515	738.397	2.054	2.509
pcGUS#19	482.939	1.979	1.397	1104.374	2.101	2.492
dsev1#6	453.999	1.979	1.391	940.336	2.07	2.518
dsev1#10	363.779	1.944	1.436	955.92	2.071	2.518
dsev1#11	478.581	2.048	1.604	1239.005	2.08	2.531
dsev1#13	475.529	1.979	1.389	921.93	2.11	2.511
dsev1#17	656.165	1.875	1.157	1752.424	2.151	2.482
dsev1#18	418.152	1.912	1.328	937.48	2.081	2.486
dsev3#1	457.796	1.94	1.376	1136.058	2.099	2.512
dsev3#3	473.919	1.982	1.381	1123.763	2.103	2.496
dsev3#4	376.286	1.992	1.437	853.106	2.137	2.395
dsev3#5	473.125	1.95	1.264	1126.963	2.113	2.508
dsev3#9	407.474	1.96	1.391	965.993	2.068	2.493
dsev3#14	572.548	1.893	1.194	933.624	2.132	2.43
dsev3#16	659.631	1.89	1.185	1249.66	2.123	2.476
dsev3#18	438.323	1.996	1.433	885.308	2.082	2.536
dsev3#19	508.874	1.963	1.297	1065.074	2.091	2.5

dsev5#1	412.621	2.038	1.561	1041.562	2.085	2.492
dsev5#4	351.945	2.068	1.572	981.552	2.073	2.52
dsev5#6	539.268	1.947	1.339	1115.441	2.075	2.513
dsev5#7	435.408	2.053	1.592	1229.758	2.074	2.479
dsev5#11	382.91	2.03	1.542	1158.128	2.076	2.513
dsev5#13	453.493	1.969	1.417	1107.369	2.071	2.503
dsev5#16	259.517	2.035	1.951	933.227	2.073	2.513
dsev5#20	389.639	2.065	1.585	1090.237	2.1	2.515
pcev2#1	441.799	2.055	1.539	922.904	2.091	2.517
pcev2#2	463.398	2.03	1.467	887.679	2.104	2.464
pcev2#3	459.452	1.981	1.397	898.28	2.093	2.47
pcev2#5	440.869	2.015	1.433	752.884	2.069	2.5
pcev2#10	669.711	1.895	1.248	1025.968	2.097	2.501
pcev2#11	433.402	2.013	1.413	1048.545	2.13	2.499
pcev2#19	392.627	2.053	1.526	662.178	2.106	2.539

Table 4. Nanodrop results for DNA extracted from uninfected *A. thaliana* leaves. Extracted using the CTAB method as described in Kiss *et al.* (2024). ds: double stranded, pc: paperclip. For WT, T: top row, M: middle row, B: bottom row.

Uninfected DNA				
Sample Name	**Infected leaf #**	**Nucleic Acid(ng/uL)**	**A260/A280**	**A260/A230**
WT#T5	T9/10	1146.131	2.079	2.087
WT#T9	T17/18	1634.255	2.147	2.218
WT#M1	M1/2	1611.229	2.136	2.203
WT#M5	M9/10	786.884	2.107	2.041
WT#M6	M11/12	1264.496	2.12	2.2
WT#M9	M17/18	1503.716	2.135	2.145
WT#B7	M13/14	1143.601	2.114	2.168
WT#B8	M15/16	605.317	2.144	2.047
dsGUS#2	3/4	825.405	2.105	2.152
dsGUS#5	9/10	1327.182	2.146	2.207
dsGUS#8	15/16	1535.343	2.137	2.238
dsGUS#9	17/18	1688.99	2.137	2.237
dsGUS#10	19/20	1324.758	2.135	2.251
pcGUS#1	1/2	733.426	2.108	2.122
pcGUS#2	3/4	1229.243	2.131	2.194
pcGUS#3	5/6	447.296	2.127	2.218
pcGUS#5	9/10	1524.043	2.135	2.274
pcGUS#7	13/14	2103.192	2.153	2.223
pcGUS#10	19/20	863.826	2.117	2.162
dsev1#3	5/6	1274.496	2.129	2.255
dsev1#4	7/8	2070.386	2.158	2.215
dsev1#5	9/10	799.259	2.109	2.173

dsev1#6	11/12	1075.204	2.126	2.256
dsev1#7	13/14	1804.612	2.133	2.254
dsev1#9	17/18	997.55	2.095	2.037
dsev3#1	1/2	1012.536	2.117	2.203
dsev3#2	3/4	1442.536	2.122	2.098
dsev3#3	5/6	618.706	2.154	2.179
dsev3#5	9/10	1186.705	2.136	2.237
dsev3#7	13/14	791.78	2.089	2.211
dsev3#8	15/16	1149.243	2.152	2.206
dsev3#9	17/18	1980.971	2.135	2.281
dsev3#10	19/20	1803.148	2.131	2.24
dsev5#1	1/2	1450.043	2.13	2.253
dsev5#3	5/6	1824.153	2.145	2.235
dsev5#4	7/8	1166.306	2.11	2.208
dsev5#2	3/4	1372.849	2.131	2.254
dsev5#6	11/12	2171.077	2.173	2.243
dsev5#7	13/14	1928.723	2.155	2.276
dsev5#8	15/16	997.7	2.136	2.257
dsev5#10	19/20	1866.663	2.161	2.273
pcev2#1	1/2	1470.144	2.147	2.193
pcev2#2	3/4	795.993	2.128	2.238
pcev2#3	5/6	1144.561	2.134	2.25
pcev2#5	9/10	1612.056	2.137	2.349
pcev2#6	11/12	1482.855	2.139	2.319
pcev2#10	19/20	832.699	2.112	2.281